Optik - International Journal for Light and Electron Optics 237 (2021) 166760

Contents lists available at ScienceDirect

Optik

journal homepage: www.elsevier.com/locate/ijleo

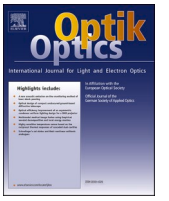

Original research article

The effect of target position on Al plasma characteristics induced by a 355 nm nanosecond laser in the presence of an external non-uniform magnetic field

Lisheng Liu [a], Junfeng Shao [a], Shuang Cui [a], Xun Gao [b,*]

[a] State Key Laboratory of Laser Interaction with Matter & Innovation Laboratory of Electro-Optical Countermeasures Technology, Changchun Institute of Optics, Fine Mechanics and Physics, Chinese Academy of Sciences, Changchun 130033, China
[b] School of Science, Changchun University of Science and Technology, Changchun 130022, China

ARTICLE INFO

Keywords:
Laser induced plasma
Spectral enhancement
Magnetic field
Target position

ABSTRACT

In this work, the effect of target position on Al plasma characteristics induced by a 355 nm nanosecond laser in the presence of an external non-uniform magnetic field was investigated by using the optical emission spectroscopy and fast imaging. The time-resolved spectra were recorded at various sample positions within the magnetic field at different time delays. It was observed that all spectral lines emitted from the Al ions or neutral atoms were enhanced in the presence of the magnetic field, and the emission intensity reached its maximum peak at delay time of 150 ns for Al II 281.6 nm and delay time of 600ns for Al I 394.6 nm. At the early stage of plasma plume expansion, the plasma plume front at M position is longer than that of at B position. As the delay time increasing, under the confinement of magnetic pressure, the plasma plume fronts for two position are near same. The observed differences in emission intensity at the various positions were attributed to the curvature and gradient of the magnetic field.

1. Introduction

Laser-induced plasmas represent a new subject of study related to electromagnetic interaction with macroscopic matter. Since the last few decades, a lot of developments have been achieved in laser plasma physics both in terms of theoretical and experimental studies [1,2]. The dynamics of laser produced plasma is effected significantly by introducing an external magnetic field and therefore it is useful to control the external parameters of plasma [3]. The use of a magnetic field during the expansion of laser-produced plasma can lead to several interesting physical phenomena such as the conversion from thermal to kinetic energy in the plasma, plume confinement, ion acceleration, emission enhancement, and plasma instability [4–6]. Studying the dynamics of laser-produced plasma with a magnetic field facilitates a better understanding of the propagation of the charged particle beams, bipolar flows associated with young stellar objects, interaction of solar winds with planetary atmospheres, formation of jets, etc [7]. The emission intensity from various species has been observed to be higher in the presence of an external field because of the magnetic confinement of the plasma [8]. In recent years, the interactions between laser-produced plasma and magnetic fields has been the subject of many researches because of its potential applications in thin film deposition [9], development of extreme ultraviolet (XUV) lithography [10], debris mitigation [11], and analytical detection limit enhancement in laser-induced breakdown spectroscopy (LIBS) [12].

* Corresponding author.
E-mail address: lasercust@163.com (X. Gao).

https://doi.org/10.1016/j.ijleo.2021.166760
Received 5 February 2021; Accepted 12 March 2021
Available online 15 March 2021

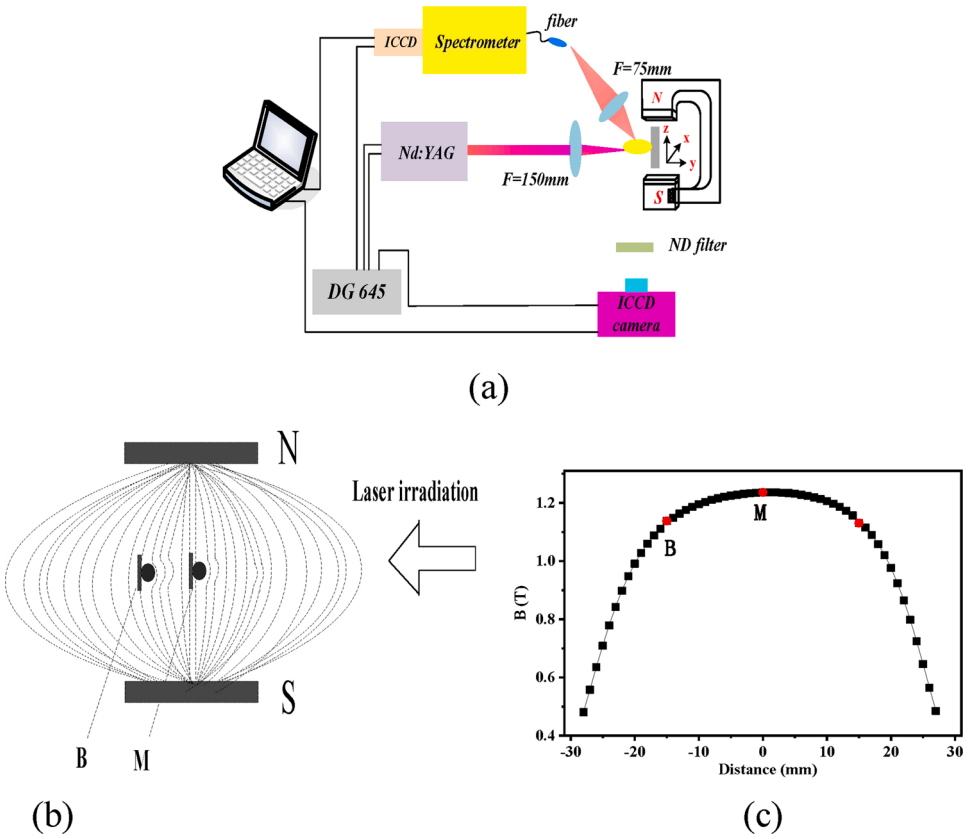

Fig. 1. (a) Schematic diagram of the experimental setup used for optical emission spectroscopy and fast imaging. (b) The positions of the sample (B and M) inside the magnetic field. (c) The magnetic field strength distribution.

Previous works based on laser-produced plasma with a magnetic field have been conducted to study enhancement effects, the improvement in LIBS sensitivity, and laser ablation applications at different positions in the magnetic field. For example, Neogi et al. [13] studied the intensity enhancement of carbon emission in the presence of a curved magnetic field, attributing the emission characteristics of carbon plasma to the curvature gradient drift. According to another report by Neogi et al. [14], a double peak structure was observed in the temporal profile of the carbon emitting species in the presence of a non-uniform magnetic field, which could be attributed to the Rayleigh-Taylor instability. Harilal et al. [15] described the influence of a transverse magnetic field on laser-induced Al plasma, and their spectroscopic studies revealed an increased emission from multiply charged ions, while the emission intensities from singly charged ions and neutral species were considerably reduced. Hussain et al. [16] investigated the influence of air gas pressures on the expansion features of nanosecond laser ablated aluminum plasma in the absence and presence of a non-uniform magnetic field using fast photography. Despite such efforts, few studies have been conducted to investigate the emission aspects and evolution dynamics of plasma plumes for different sample positions in an external magnetic field.

In the present work, the emission features and expansion dynamics of laser-produced Al plasma at different positions in a non-uniform external magnetic field have been characterized using optical emission spectroscopy and fast imaging. The third harmonic generation of the Nd:YAG laser (355 nm) has been employed to generate the Al plasma in air atmosphere. Two parallel permanent magnets with maximum intensity at the center and decreasing intensity on either side have been used to apply a non-uniform magnetic field on the expanding plasma.

2. Experimental setup

Fig. 1 shows a schematic layout of the experimental setup used for performing the optical emission spectroscopy and fast imaging analysis. The laser pulse from the Nd:YAG laser (Continuum, Power 8000) emitting an pulsed energy of 200 mJ in the third harmonic generation mode (355 nm) with a pulse duration of 7 ns and a repetition rate of 10 Hz was employed to induced Al plasma in the experiment. The laser beam was focused onto the Al target surface with the dimensions 30 mm × 30 mm × 2 mm by using a quartz lens with the focal length of 100 mm, and the laser beam ablate size on the Al target surface is 200 μm.

Before laser ablation, the Al target surface is ground and cleaned with acetone to remove any contamination. The Al sample is mounted on an XYZ translation stage to provide a fresh surface for the next laser pulse. The optical emission spectroscopy from the Al plasma are collected on an optical fiber using a 75-mm focal length convex lens, and then coupled with an optical spectrograph

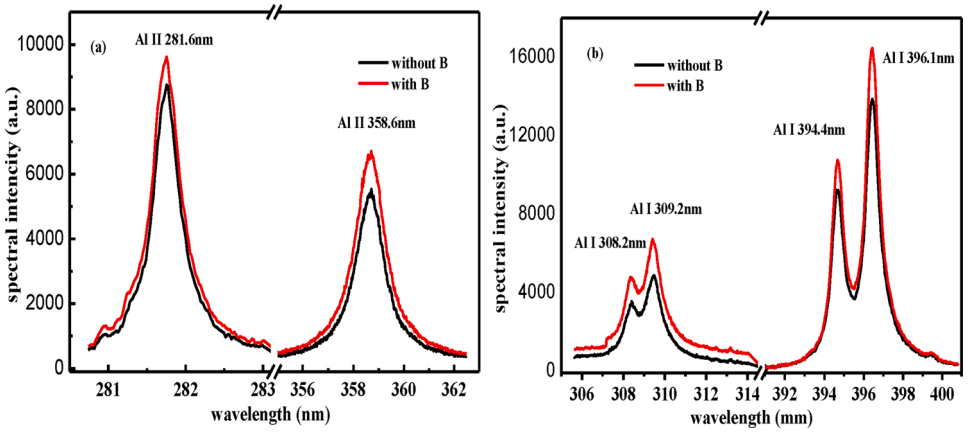

Fig. 2. Emission spectrum of the laser-produced Al plasma with and without a magnetic field. (a) Al ionize emissions (281.6 nm and 358.6 nm); (b) Al atomic emissions (Al 308.2 nm, 309.2 nm, 394.4 nm and 396.1 nm).

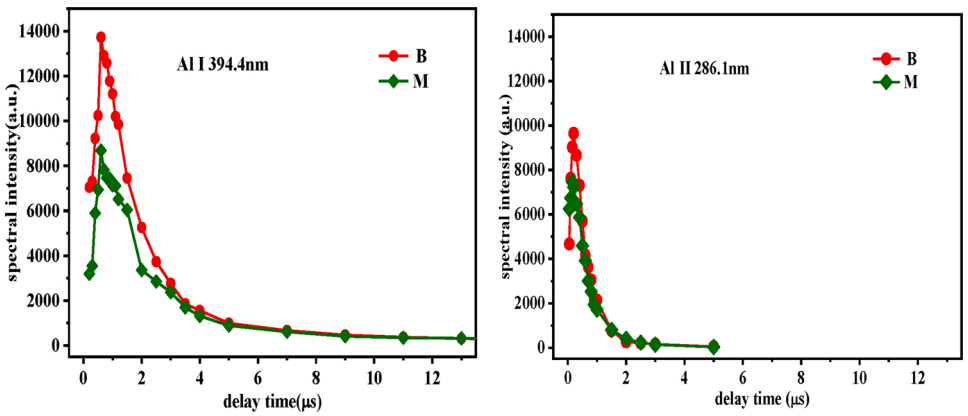

Fig. 3. Temporal resolution of aluminum plasma at two sample positions, B and M: (a) 394.4 nm, (b) 281.6 nm.

equipped with 1200 line/mm diffraction gratings. An intensified charge coupled device (ICCD) was attached to the spectrograph. The visible and ultraviolet radiations from the plasma emission were recorded integrally in the 390–410 nm and 270–300 nm wavelength ranges with a spectral resolution of ±0.05 nm. A digital pulse delay generator (DG645) was used to synchronously trigger the laser and the ICCD detector.

For fast imaging of the plasma plume, a Nikon camera lens (100 mm, f/2.8) was used to image the plasma plume onto the an ICCD camera (Andor DH334,1024 × 1024 pixels) to acquire a two-dimensional image. The plasma plume images were taken from the side of the plasma plume with a magnification of 1:2. To prevent over-exposure, neutral attenuation plates were placed in front of the ICCD camera. It should be noted that all the fast images were taken at 10 % gate width of delay times. Data acquisition and subsequent analyses were performed on a personal computer.

The transverse magnetic field was applied using a pair of 65 mm × 55 mm × 15 mm permanent magnets placed at a parallel distance of 16 mm from each other. The maximum magnetic field measured with a Gauss device at point M was observed to be 1.23 T, which was similar to the field intensity observed at B positions (1.13 T) as shown in Fig. 1(b). Point M represents the mid position and the B position is at a distance of 15 mm from point M along the x-axis. The external magnetic field intensity was maximum at M and decreased on either side along the x-axis as shown in Fig. 1(c). The Al surface was placed in between the poles at two different positions with respect to B and M as shown in Fig. 1(b). All experimental measurements were performed at 1.0 atm in ambient air and at a room temperature of 300 K.

3. Results and discussion

The Al plasma spectrum was obtained at point M inside the magnetic field. Fig. 2 shows the time-integrated emission spectra recorded in the absence and presence of a magnetic field at a detection distance of 5 mm from the Al sample's surface. The spectra were collected at a gate delay of 500 ns and the gate width was fixed to 100 ns in both cases. In Fig. 2(a) and (b) two Al ion lines at Al II 281.6 nm (3s4s–3s3p) and Al II 358.6 nm (3s4f–3s3d) and four Al neutral emission lines at Al I 308.2 nm ($3s^2 3d–3s^2 3p$), 309.2 nm

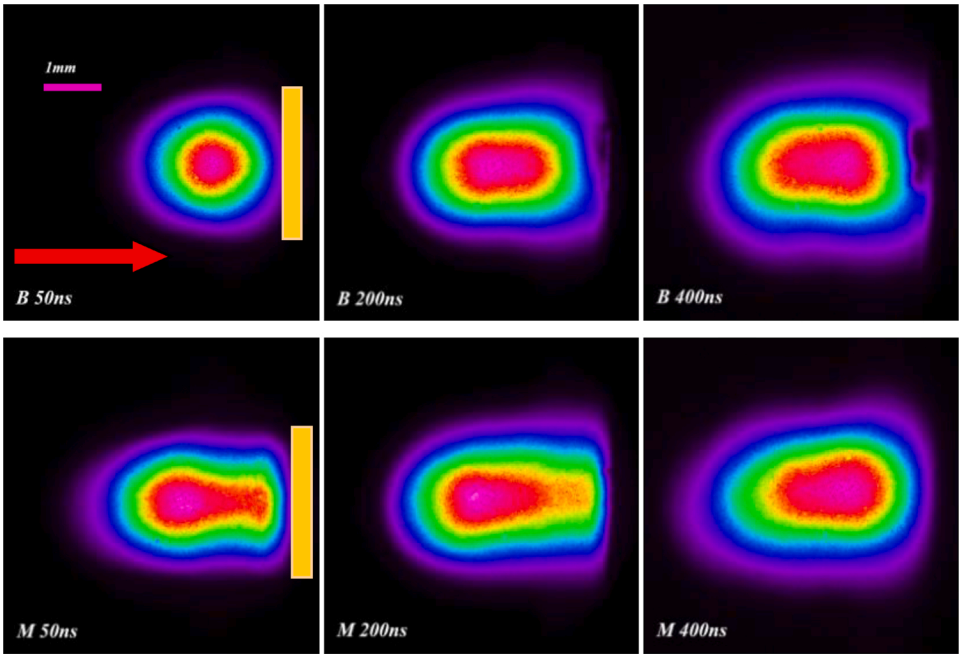

Fig. 4. Images of the time evolution of the plumes of Al plasmas in the presence of a magnetic field at three time delays; the sample was placed at two positions (B and M).

($3s^2 3d–3s^2 3p$), 394.4 nm ($3s^2 4s–3s^2 3p$), and 396.1 nm ($3s^2 4s–3s^2 3p$) were observed, respectively. There was a significant spectral enhancement for the Al ionize (Al II 281.6 nm and Al II 358.6 nm)and Al atomic(Al I 308.2 nm, Al I 309.2 nm, Al I 394.4 nm, and Al I 396.1 nm) emission lines when the plume expanded across the external magnetic field.

To understand the dynamics of laser-produced plasma and its emissions, the temporal evolution of the atomic and ionic lines for Al I 394.6 nm and Al II 281.6 nm are recorded at various time delays. During the temporal resolution measurement, the Al sample is placed in two positions between the magnetic poles (labeled as B and M) as shown in Fig. 1(b). Fig. 3(a) and (b) show the temporal resolution of atomic and ionic lines as a function of the delay time in the presence of a magnetic field at two sample positions, B and M, for the emission spectral intensities of 394.6 nm and 281.6 nm.

At an initial delay time of 50 ns, the atomic and the ionic emission lines all appeared, and their intensity increased initially and then decreased with the increasing in the delay time as shown in Fig. 3, the emission intensity reached its maximum peak at delay time of 150 ns for Al II 281.6 nm and delay time of 600 ns for Al I 394.6 nm. The spectral intensities of 394.6 nm and 281.6 nm in the presence of magnetic field was higher at the B position than for the M positions, which attributed from the plasma interaction with magnetic field. The lifetime of the ionic line was shorter than the atomic line in the presence of a magnetic field, however, the lifetime of the atomic line wasn't almost changed in the presence of a magnetic field, because the atomic number density was unchanged. These observations are in strong agreement with previously published results by Neogi et al. [14] for laser-produced carbon plasma across different regions of a curved magnetic field; they reported that the curvature and gradient of the magnetic field was responsible for different phenomena. The magnetic field lines were more compressed and convex at position B and hence moved the plasma with a positive field gradient, in contrast to other position in the magnetic fled where the field lines were concave and moved the plasma with a negative field gradient.

In a curved field, the drift experienced by the charged species because of the curvature and gradient of the magnetic field is given by

$$\upsilon_{\mathrm{d}} = \upsilon_R + \upsilon_{\nabla B} = \frac{m}{q}\frac{R_c \times B}{R_c^2 B^2}\left(\upsilon_{//}^2 + \frac{1}{2}\upsilon_{\perp}^2\right) \tag{1}$$

where υ_R and $\upsilon_{\nabla B}$ is are the drift due to curvature and the gradient of the magnetic field, respectively, $\upsilon_{//}$ and $\upsilon_{\perp}$ denote velocity parallel and perpendicular to the magnetic lines of force, R_c is the radius of curvature, and B is the magnetic field. Since the mass of the electron is smaller than that of ions, the movement of ions due to electromagnetic force can be neglected. By contrast, electron drift due to the curvature of the magnetic field can be neglected when compared with ionic drift. The electrons and ions moved in the same direction at position B compared to position M where their movement was in the opposite direction because of the change in the direction of the radius of curvature. Thus, because of the distortion of the field lines, the effective magnetic pressure and $J \times B$ force was highest at B position compared with M position; the electron-ion collision frequency also increased resulting in the highest intensity spectral line. This could explain the comparatively lower spectral intensity observed at M position.

To understand the hydrodynamics of the plasma plumes, a fast imaging study was performed at various time delays in the presence of a magnetic field at three different sample locations. Fig. 4 shows the plume dynamics (2-dimensional images) of laser-produced Al

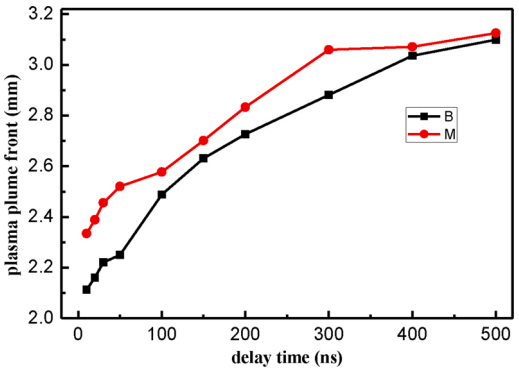

Fig. 5. Plume front position of the Al plasma at three different positions (B and M) in the presence of a magnetic field.

plasma for two sample positions (B and M) at different time delays with respect to the ablating pulse in the presence of a magnetic field. These fast images were recorded at time delays of 50, 200 and 400 ns for each position in the field. As shown in Fig. 4, the plasma sample at position B not only propagated in the direction of the laser beam, but also contained a lateral expansion part. At position M, the plume's forward motion was fast with a near hemispherical geometry. This was because the pressure within the plume and the initial density gradients pushed the plasma perpendicular to the sample surface instead of the radial direction.

Fig. 5 shows the plume front evolution of the plasma at three sample positions in the field as a function of time delays. The observed plume front extension of Al plasma in the magnetic field at two different locations increased with the increase in the time delay. At the early stage of plasma plume expansion, the plasma plume front at M position is longer than that of at B position. As the delay time increasing, under the confinement of magnetic pressure, the plasma plume fronts for two position are near same. Comparing Figs. 3 and 5, we observed an increase in the magnetic confinement of the plasma emission and a deceleration in plasma expansion at the two sample positions. At position B, because the plasma expansion was in the same direction as the curvature and gradient, the magnetic pressure was higher, electron-ion collision frequency increased, ohmic heating increased, plasma expansion velocity decreased, plasma plume front reduced, and plasma emission increased compared with another position.

4. Conclusion

In this work, the time-integrated spectra and expansion dynamics of laser-produced aluminum plasma in different regions of a magnetic field was presented. The optical emission in the presence of a magnetic field showed enhancement because of either the Al ions or the neutral atoms. The temporal profiles of the neutral and ionic species showed distinct features with respect to the position of the sample in the magnetic field. It was observed that the curvature and gradient of the magnetic field significantly altered the intensity. The effect of the sample position on the expanding Al plasma was also studied using fast photography analysis. The imaging results revealed that the sample position significant influenced the morphology of the plasma plumes.

Declaration of Competing Interest

The authors declared that they have no conflicts of interest to this work. We declare that we do not have any commercial or associative interest that represents a conflict of interest in connection with the work submitted.

Acknowledgments

This project was supported by National Nature Science Foundation of China [Grant No. 61575030] and the National Key Laboratory of laser matter interaction (Grant No. SKLLIM1905).

References

[1] A. Bogaerts, Z.Y. Chen, D. Autrique, Double pulse laser ablation and laser induced breakdown spectroscopy:A modeling investigation, Spectrochim. Acta Part B 63 (2008) 746–754.
[2] J.J. Camacho, M. Santos, L. Diaz, J.M.L. Poyato, Optical emission spectroscopy of oxygen plasma induced by IR CO2 pulsed laser, J. Phys. D Appl. Phys. 41 (2008) 215206.
[3] S. Suckewer, C.H. Skinner, H. Milchberg, C. Keane, D. Voorhees, Amplification of stimulated soft x-ray emission in a confined plasma column, Phys. Rev. Lett. 55 (17) (1985) 1753.
[4] H.B. Tang, G.Y. Hu, Y.H. Liang, T. Tao, Y.L. Wang, P. Hu, B. Zhao, J. Zheng, Confinement of laser plasma expansion with strong external magnetic field, Plasma Phys. Control. Fusion 60 (5) (2018), 055005.
[5] Y. Li, C.H. Hu, H.Z. Zhang, Z.K. Jiang, Z.S. Li, Optical emission enhancement of laser-produced copper plasma under a steady magnetic field, Appl. Opt. 48 (4) (2009) B105–B110.
[6] D.B. Zhang, Y.F. Xu, S.J. Wang, Quasilinear transport due to the magnetic drift resonance with the ion temperature gradient instability in a rotating plasma, Phys. Plasmas 24 (8) (2017), 082306.

[7] A.N. Mostovych, B.H. Ripin, J.A. Stamper, Laser produced plasma jets: collimation and instability in strong transverse magnetic fields, Phys. Rev. Lett. 62 (24) (1989) 2837.
[8] C. Lu, X. Gao, Q. Li, C. Song, J.Q. Lin, Spectral enhancement of laser-induced breakdown spectroscopy in external magnetic field, Plasma Sci. Technol. 17 (11) (2015) 919–922.
[9] M.S. Tillack, D.W. Blair, S.S. Harilal, The effect of ionization on cluster formation in laser ablation plumes, Nanotechnology 15 (2004) 390–403.
[10] A. Roy, S.M. Hassan, S.S. Harilal, A. Endo, T. Mocek, A. Hassanein, Extreme ultraviolet emission and confinement of tin plasmas in the presence of a magnetic field, Phys. Plasmas 21 (5) (2014), 053106.
[11] S.S. Harilal, M.S. Tillack, Y. Tao, B. O'Shay, R. Paguio, A. Nikroo, Extreme-ultraviolet spectral purity and magnetic ion debris mitigation by use of low-density tin targets, Opt. Lett. 31 (10) (2006) 1549–1551.
[12] S.A. Abbasi, Z. Aziz, T.M. Khan, D. Ali, T. Hassan, J. Iqbal, S.U.D. Khan, A. Ahmad, R. Khan, E.M. Khan, Enhancement of optical signal and characterization of palladium plasma by magnetic field-assisted laser-induced breakdown spectroscopy, Optik 224 (2020) 165746.
[13] A. Neogi, R.K.T. hareja, Laser-produced carbon plasma expanding in vacuum, low pressure ambient gas and nonuniform magnetic field, Phys. Plasmas 6 (1) (1999) 365–371.
[14] A. Neogi, R.K. Thareja, Dynamics of laser produced carbon plasma expanding in a nonuniform magnetic field, J. Appl. Phys. 85 (1999) 1131–1136.
[15] S.S. Harilal, M.S. Tillack, B. O'Shay, C.V. Bindhu, F. Najmabadi, Confinement and dynamics of laser-produced plasma expanding across a transverse magnetic field, Phys. Rev. E 69 (2) (2004), 026413.
[16] A. Hussain, X. Gao, Q. Li, Z.Q. Hao, J.Q. Lin, Combined effects of ambient gas pressures and magnetic field on laser plasma expansion dynamics, Plasma Sci. Technol. 19 (1) (2017), 015505.